Neuron
Review

Signal Processing in the Axon Initial Segment

Maarten H.P. Kole[1,2] and Greg J. Stuart[1,*]
[1]John Curtin School of Medical Research, Australian National University, ACT 0200, Australia
[2]Netherlands Institute for Neuroscience, Meibergdreef 47, 1105 BA Amsterdam, The Netherlands
*Correspondence: greg.stuart@anu.edu.au
DOI 10.1016/j.neuron.2012.01.007

The axon initial segment (AIS) is a specialized membrane region in the axon of neurons where action potentials are initiated. Crucial to the function of the AIS is the presence of specific voltage-gated channels clustered at high densities, giving the AIS unique electrical properties. Here we review recent data on the physiology of the AIS. These data indicate that the role of the AIS is far richer than originally thought, leading to the idea that it represents a dynamic signal processing unit within neurons, regulating the integration of synaptic inputs, intrinsic excitability, and transmitter release. Furthermore, these observations point to a critical role of the AIS in disease.

Introduction

The axon of neurons in the mammalian central nervous system (CNS) contains a specialized region called the axon initial segment (AIS). This denotes a thin unmyelinated region of axon (10–60 μm in length) between its origin at the axon hillock, typically near the cell body, and the beginning of myelination (Figure 1A). Unmyelinated axons also contain an AIS, which, as with myelinated axons, can be identified by the expression of high densities of specific ion channels and associated proteins. At the electron microscopic level the AIS is characterized by a dense granular layer beneath the surface membrane, which is not found at the soma, and is similar to that at nodes of Ranvier (Figure 1B) (Palay et al., 1968; Peters et al., 1968). While the molecular composition of this granular layer is not fully understood, by analogy with nodes of Ranvier it is thought to contain a high density of voltage-gated channels together with specialized anchoring proteins important for action potential generation. In addition, the AIS of some neuronal cell types, such as cortical pyramidal neurons, receives synaptic input (Figure 1) (Somogyi et al., 1998).

Experiments in the 1950s proposed that action potentials (APs) are initiated in the proximal axon, at either the axon hillock (Fuortes et al., 1957) or the initial segment (Araki and Otani, 1955; Coombs et al., 1957). Aided by advances in electrical and optical recording techniques, recent data have provided direct evidence in support of these early observations, showing that APs are initiated at the distal end of the AIS in a large range of neuronal cell types. These studies have in addition revealed that the AIS is not just a trigger zone for AP generation, but also plays a key role in regulating the integration of synaptic input, as well as intrinsic excitability and transmitter release.

In this review we focus on the detailed electrical properties of the AIS and describe how these unique properties influence synaptic integration and shape neuronal output. We refer the reader to excellent recent reviews on the physiology of the axon proper and the molecular structure of the AIS (Debanne et al., 2011; Rasband, 2010).

Evolution of the AIS and Channel Targeting

While it has long been thought that APs are initiated in the AIS of neurons in the mammalian CNS, this is not the case in all species. For instance, multipipette recording and voltage-sensitive dye imaging indicate that AP initiation in invertebrate neurons can occur at multiple locations, which can act independently (Calabrese and Kennedy, 1974; Maratou and Theophilidis, 2000; Meyrand et al., 1992; Tauc, 1962; Zecević, 1996). These studies indicate that invertebrate neurons lack the functional polarization found in neurons of the mammalian CNS (Rasband, 2010). It is therefore relevant to ask why and when in evolution did neurons develop an AIS, thereby defining a single locus for AP generation?

Insights into the evolution of the AIS have been obtained by studying the gene sequences of Na^+ and K^+ channels, which are localized to the AIS via an interaction with the cytoskeletal scaffolding protein Ankyrin G. Ankyrin G, widely used as a marker for the AIS, is restricted in expression to the AIS and nodes of Ranvier and required for targeting of voltage-gated Na^+ channels to the AIS (Kordeli et al., 1995; Zhou et al., 1998). This occurs via an interaction between Ankyrin G and a conserved nine amino acid sequence in the II-III domain of Na^+ channels (Garrido et al., 2003). The same binding motif has been found in K_v7 K^+ channels that, similar to Na^+ channels, cluster at the AIS and nodes of Ranvier (Devaux et al., 2004; Pan et al., 2006). In order to map the evolution of the AIS, Hill et al. (2008) made an elegant comparative study of the gene sequences of Na^+ and K_v7 channel anchoring motifs in chordates, nonchordates, and vertebrates. Their results show that while anchoring motifs in Na^+ channels are highly conserved and found as early as the chordates, the first immunohistological observations of Na^+ channel clustering in axons occurs only with the appearance of the vertebrates, such as the lamprey. In contrast, the anchoring motif in K_v7 channels developed 50 to 100 million years later, at the same time as the appearance of axon myelination (Hartline and Colman, 2007). This suggests that the formation of the AIS preceded the evolution of myelination and coincided with the appearance of complex sensory systems in vertebrates. Furthermore, these studies suggest there are parallels in the molecular evolution of the AIS and the transition to a single site for AP initiation in neurons. We next address the issue of what types of proteins are specifically expressed in the AIS and their role in excitability.

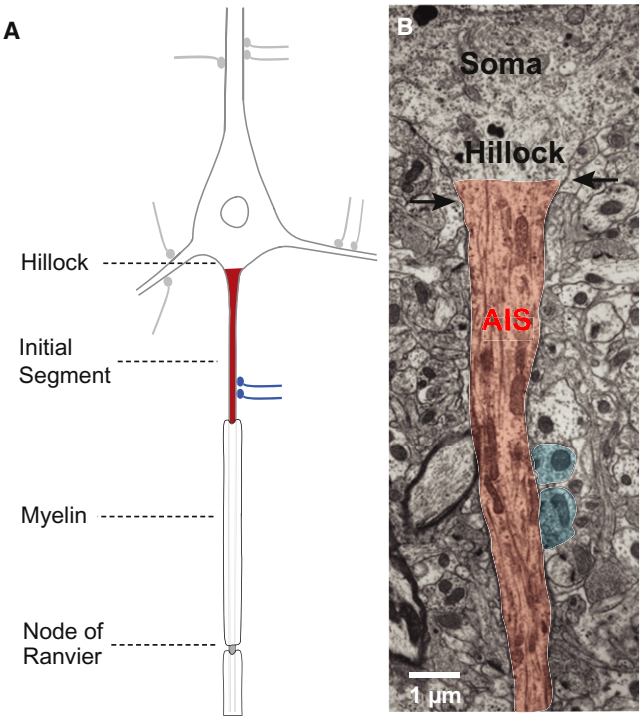

Figure 1. Anatomy of the Axon Initial Segment

(A) Schematic of a pyramidal neuron axon showing the location of the hillock, initial segment (AIS; red), and axon proper. Synaptic input onto the AIS is shown in blue.

(B) Electron micrograph of the AIS of a cortical pyramidal neuron. The soma, axon hillock, and AIS (red) are indicated. Blue areas indicate presynaptic terminals onto the AIS. Arrows (black) indicate the onset of the dense granular layer beneath the surface membrane indicating the start of the AIS. Adapted from Peters et al. (1968).

Ion Channels in the AIS

Na^+ Channels

Na^+ channels provide the main transient inward current responsible for the rapid depolarizing phase of the AP (Hodgkin and Huxley, 1952). Early computational modeling studies predicted that initiation of APs in the AIS required a high concentration of Na^+ channels (Dodge and Cooley, 1973). Consistent with this, initial binding studies indicated that the density of Na^+ channels in the AIS of cultured spinal cord neurons and retinal ganglion cells is indeed high (Catterall, 1981; Wollner and Catterall, 1986).

We now know that of the four Na^+ channel α-subunits expressed in the brain ($Na_v1.1$, $Na_v1.2$, $Na_v1.3$, and $Na_v1.6$), three subtypes ($Na_v1.1$, $Na_v1.2$, and $Na_v1.6$) are localized to the AIS with developmental, regional, and cell-type-specific diversity (see Table 1). Immunocytochemical studies indicate that the main Na^+ channel isoform found in the AIS of neurons in the adult CNS is $Na_v1.6$ (Figure 2A). The $Na_v1.1$ subtype is also found in the AIS of GABAergic interneurons, retinal ganglion cells, and spinal cord neurons (Duflocq et al., 2008; Lorincz and Nusser, 2008, 2010; Ogiwara et al., 2007; Van Wart et al., 2007). $Na_v1.2$ is primarily expressed in the AIS early in development and in adults in unmyelinated axons (Jarnot and Corbett, 1995; Boiko et al., 2003), but has also been reported in the proximal part of the AIS of pyramidal neurons from the cortex and hippocampus (Hu et al., 2009).

While these immunocytochemical studies provided strong evidence for a high Na^+ channel density in the AIS, initial functional experiments using patch-clamp recording surprisingly reported that the Na^+ current density in the AIS was similar to that at the soma (Colbert and Johnston, 1996; Colbert and Pan, 2002). More recent electrophysiological experiments, however, back up the idea that the AIS Na^+ channel density is indeed significantly higher than at the soma (Figure 2B). The discrepancy with earlier estimates is best explained by an inability to draw AIS Na^+ channels into the patch-clamp recording pipette due to tight coupling of these channels to the actin cytoskeleton (Kole et al., 2008). Consistent with this idea, much larger Na^+ currents are observed in patch-clamp recordings from the AIS after chemical disruption of the actin cytoskeleton (Kole et al., 2008) and in recordings from axon blebs (Hu et al., 2009; Schmidt-Hieber and Bischofberger, 2010). Axonal blebs are swellings where the axon has been cut at the surface of the brain slice and then sealed over and, therefore, presumably do not have an intact cytoskeleton (Hu et al., 2009). As they are larger than the axon they provide a more accessible location for making axonal recordings (Shu et al., 2006). In addition, disruption of myelination at the cut end allows one to record from myelinated axons at locations that would otherwise not be possible. While recording from axon blebs has technical advantages, it should be recognized that they are damaged regions of the axon. As such, channel expression at these axon structures may not be representative of that in the intact axon. Despite this caveat, these recent functional estimates suggest the AIS Na^+ channel density is indeed high ($\sim$110 to 300 channels/μm, assuming a 17 pS single-channel conductance), giving a conductance density of 2,000 to 5,000 pS/μm^2. For comparison, the Na^+ channel density in the squid giant axon is around 1,200 pS/μm^2 (Hodgkin and Huxley, 1952).

While there is now general consensus that the density of Na^+ channels is high in the AIS, whereas it is low in dendritic regions (Magee and Johnston, 1995; Stuart and Sakmann, 1994), how the density of Na^+ channels at the soma compares to that in the AIS is still debated. As mentioned above, recent electrophysiological estimates provide evidence that the density of Na^+ channels at the AIS is much higher than at the soma (see Figure 2B). Consistent with this idea, Lorincz and Nusser (2010) using quantitative freeze-fracture immunogold labeling found that the number of $Na_v1.6$ channels in the AIS of hippocampal pyramidal neurons was $\sim$40-fold higher than that found at the soma (Figure 2A2). In sharp contrast, a recent study using Na^+ dye imaging together with modeling predicted that the difference in Na^+ channel density between the AIS and the soma in cortical pyramidal neurons is only 3-fold (Fleidervish et al., 2010). Presumably, methodological differences underlie this apparent discrepancy. Immunocytochemical studies suffer from the fact that they do not provide information on functional channels, whereas channel density estimates based on Na^+ imaging rely on accurate modeling of Na^+ diffusion. Furthermore, the precise Na^+ channel density in the AIS, and how this compares to that in the soma and dendrites, is likely to vary between different neuronal cell types, due to variability in the electrical load of the somato-dendritic region, axonal morphology, and neuronal activity. Accurate determinations of Na^+ channel distributions

Table 1. Ion Channel Expression Patterns in the Axon Initial Segment

Current	Channel	Cell Type	Reference
I_{NaT}	$Na_v1.1$	IN, RGC, MN	Van Wart et al., 2007; Lorincz and Nusser, 2008; Duflocq et al., 2008
	$Na_v1.2$	PC	Hu et al., 2009; Lorincz and Nusser, 2010
	$Na_v1.6$	PC, DG, RGC, PN, IN, MN	Van Wart et al., 2007; Hu et al., 2009; Royeck et al., 2008; Boiko et al., 2003; Catterall, 1981; Inda et al., 2006; Kuba et al., 2006; Lorincz and Nusser, 2008; Lorincz and Nusser, 2010; Kress et al., 2010; Duflocq et al., 2008
I_{NaP}	$Na_v1.?$	PC	Stuart and Sakmann, 1995; Astman et al., 2006
I_D	$K_v1.1$	PC, MNTB, IN	Dodson et al., 2002; Shu et al., 2007b; Kole et al., 2007; Goldberg et al., 2008; Lorincz and Nusser, 2008
	$K_v1.2$	PC, RGC, MNTB, IN	Dodson et al., 2002; Shu et al., 2007b; Kole et al., 2007; Inda et al., 2006; Lorincz and Nusser, 2008; Van Wart et al., 2007
	$K_v2.2$	MNTB	Johnston et al., 2008
I_A	$K_v1.4$	PC	Ogawa et al., 2008
I_M	$K_v7.2$ / $K_v7.3$	PC	Pan et al., 2006; Shah et al., 2008
	$K_v7.2$	MN, DG	Devaux et al., 2004; Klinger et al., 2011
I_{Ca} (T/R-type)	$Ca_v2.3$ / $Ca_v3.2$ / $Ca_v3.1$	CC, PC, PN	Bender and Trussell, 2009
I_{Ca} (P/Q/N-type)	$Ca_v2.1$/$Ca_v2.2$	PC; PN	Callewaert et al., 1996; Yu et al., 2010

IN, interneuron; PC, pyramidal cell; DG, dentate granule cell (hippocampus); PN, Purkinje neuron; RGC, retinal ganglion cell; MNTB, medial nucleus of the trapezoid body; CC, cartwheel cell; MN, spinal cord motoneuron.

require unbiased matching of a wide range of AP properties (amplitude, rate of rise, site of initiation) in morphological realistic models. Using this approach, estimates in large cortical pyramidal neurons indicate AIS-to-soma Na^+ channel ratios of ~50-fold (Kole et al., 2008), whereas in electronically compact dentate granule cells a ~5-fold difference seems to suffice (Schmidt-Hieber and Bischofberger, 2010).

In addition to their high density, the properties of Na^+ channels in the AIS are specialized, presumably to facilitate AP initiation in the AIS. For example, the voltage dependence of both activation and inactivation of AIS Na^+ channels is hyperpolarized by ~10mV compared to Na^+ channels at the soma (Figure 2C) (Colbert and Pan, 2002; Hu et al., 2009; Kole et al., 2008). This observation is consistent with subunit-specific differences in the voltage dependence of Na^+ channels (Rush et al., 2005), providing further evidence that the primary Na^+ channel subunit in the AIS is $Na_v1.6$ (Hu et al., 2009; Lorincz and Nusser, 2010; Royeck et al., 2008). AIS Na^+ channels in dentate granule cells have also been shown to activate and inactivate approximately two times faster than those at the soma (Schmidt-Hieber and Bischofberger, 2010). This observation has been used to explain how a low density of Na^+ channels in the AIS of cortical pyramidal neurons could generate fast rising APs in the AIS (Fleidervish et al., 2010). Faster channel kinetics, however, means less charge influx per channel, leading to smaller AP amplitudes for a given Na^+ channel density. Rapid Na^+ channel kinetics alone, therefore, is unlikely to explain AP generation in the AIS, leading to the conclusion that a high density of Na^+ channels is likely to be an absolute requirement.

Another specialized property of Na^+ channels is that they can be activated at subthreshold potentials, as well as undergo incomplete inactivation, leading to generation of the so-called persistent Na^+ current (I_{NaP}) (Taddese and Bean, 2002). Presumably due to the high density of Na^+ channels in the AIS, I_{NaP} has been found to be greatest in the axon (Astman et al., 2006; Stuart and Sakmann, 1995), where it has a significant influence on AP threshold (Kole and Stuart, 2008; Royeck et al., 2008). Activation of I_{NaP} is also thought to be important for generation of the AP afterdepolarization, and as such plays a role in the generation of high-frequency AP bursts (Azouz et al., 1996). Recent data in cortical pyramidal neurons indicates that AP bursts also require I_{NaP} activation at the first node of Ranvier (Kole, 2011). Na^+ channels, and especially the $Na_v1.6$ isoform, can also undergo transient reactivation upon repolarization, leading to generation of a resurgent Na^+ current (I_{NaR}). Studies in perirhinal cortex indicate that I_{NaR} is also primarily localized to the AIS (Castelli et al., 2007). These unique properties of AIS Na^+ channels together with high levels of expression in the AIS define this site as the locus for AP generation in neurons of the vertebrate CNS.

K^+ Channels

K^+ channels are critical for AP repolarization and play a role in setting AP threshold, interspike interval, and firing frequency. The predominant K^+ channel in the AIS of most neuronal types is the low-threshold K_v1 subtype (Figure 2A1). High levels of antibody staining for $K_v1.1$ and $K_v1.2$ channels, together with auxiliary β-subunits, are found in the AIS of most neuronal types (Table 1) (Dodson et al., 2002; Goldberg et al., 2008; Inda et al., 2006; Lorincz and Nusser, 2008; Ogawa et al., 2008; Van Wart et al., 2007). Consistent with these immunocytochemical studies, direct patch-clamp recording from the AIS has revealed a high density of dendrotoxin (DTX)-sensitive, fast-activating, but slowly inactivating, K_v1-type K^+ current in the AIS of cortical pyramidal neurons (Figure 2D) (Kole et al., 2007; Shu et al., 2007b). In contrast, the AIS of cerebellar Purkinje cells, a spontaneously firing cell type, lacks K_v1 expression (Lorincz and

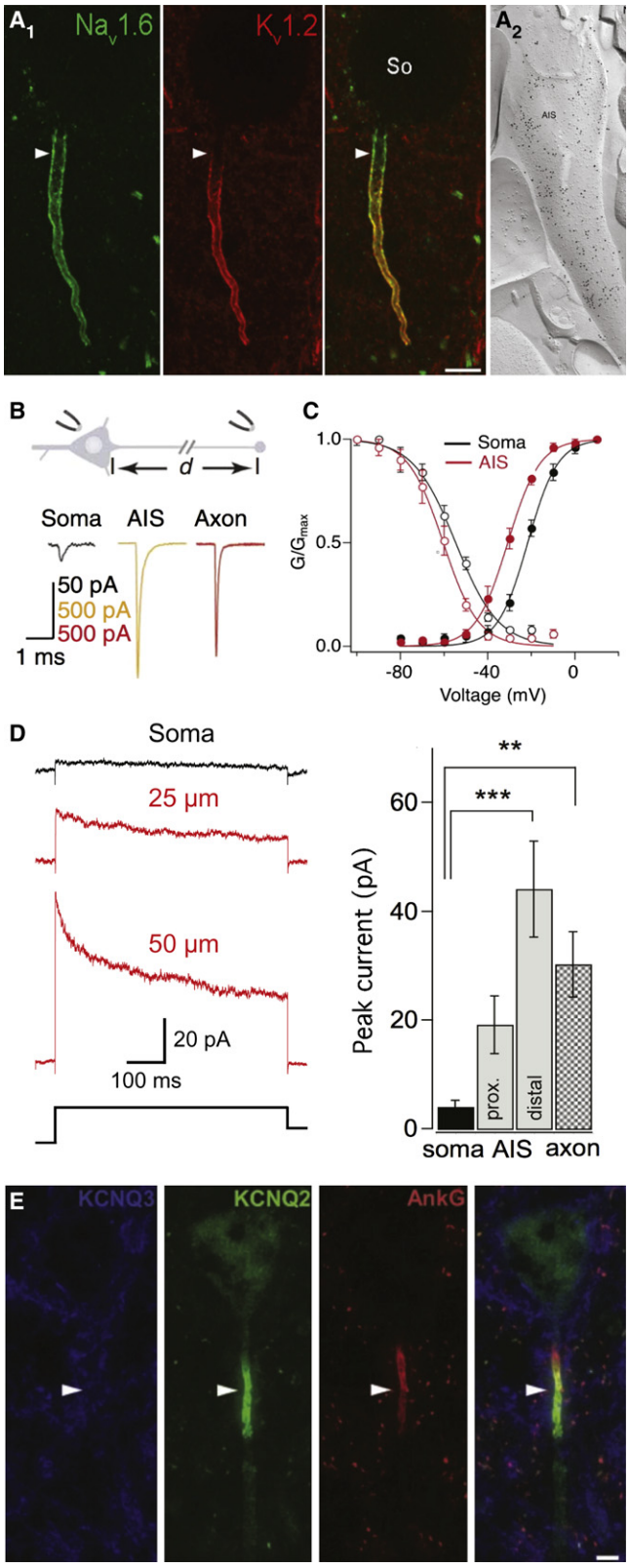

Figure 2. Ion Channel Expression in the Axon Initial Segment

(A1) Immunocytochemical staining for $Na_v1.6$ (left), $K_v1.2$ (middle), and an overlay of $Na_v1.6$ and $K_v1.2$ staining in a cortical layer 5 pyramidal neuron axon (right).

(A2) Immunogold labeling (dark spots) for $Na_v1.6$ in the AIS of a hippocampal pyramidal neuron. Adapted from Lorincz and Nusser (2008, 2010).

(B) Na^+ currents recorded in outside-out patches from the soma, the AIS, and the distal axon. AIS and distal axon recordings are from membrane blebs. Adapted from Hu et al. (2009).

(C) Comparison of the voltage dependence of activation and inactivation of somatic and AIS Na^+ channels. Data fit with the Boltzmann functions. Adapted from Kole et al. (2008).

(D) Left: K^+ currents recorded in cell-attached patches from the soma (black) and two different AIS locations (red). Right: average K^+ current at the indicated locations. Adapted from Kole et al. (2007).

(E) Immunocytochemical staining showing $K_v7.2$ staining (KCNQ2) colocalized with Ankyrin G (AnkG), but not $K_v7.3$ (KCNQ3), in the AIS of a spinal motoneuron. All three images are overlaid on the far right. Adapted from Devaux et al. (2004).

Nusser, 2008), whereas the AIS of neurons in the medial nucleus of the trapezoid body (MNTB) contains both $K_v1.2$ and $K_v2.2$ channels (Johnston et al., 2008). Antibody staining indicates that the distal part of the AIS of pyramidal neurons also contains high densities of $K_v7.2$ and $K_v7.3$ channels (Figure 2E, Table 1) (Devaux et al., 2004; Pan et al., 2006). These channels generate a slowly activating and noninactivating M-type current (Brown and Passmore, 2009).

Ca^{2+} Channels

It has long been recognized that organelles sequestering Ca^{2+} are localized to the AIS of pyramidal neurons from the neocortex and hippocampus (Peters et al., 1968). These endoplasmatic reticulum (ER)-like organelles are positioned close to the cell membrane, contain Ca^{2+} ATPase-type Ca^{2+} pumps, and are thought to be equivalent to the spine apparatus (Bas Orth et al., 2007). One obvious function of these organelles would be to sequester calcium that locally enters the AIS via voltage-gated Ca^{2+} channels. Consistent with this idea, P/Q-type Ca^{2+} channels are present in the AIS of cerebellar Purkinje (Callewaert et al., 1996) and neocortical pyramidal neurons (which also contains N-type Ca^{2+} channels), whereas the AIS of GABA-ergic interneurons from the dorsal cochlear nucleus contains R- and T-type Ca^{2+} channels (Bender and Trussell, 2009; Yu et al., 2010).

Together, these data indicate that while there are general rules, the expression patterns of different ion channels in the AIS are highly cell specific. A summary of these expression patterns in different neuronal cell types can be found in Table 1.

Signal Processing in the AIS

The large diversity of voltage-gated ion channel expression in the AIS is likely to play a fundamental role in how different neuronal cell types transform synaptic inputs into output signals. Recent electrophysiological recordings from the AIS, as well as voltage-sensitive dye imaging studies, have provided direct evidence that APs are initiated at the distal end of the AIS. In addition, they have revealed that the AIS processes synaptic inputs in complex ways, which, due to its electrical isolation, can occur independently of signal processing in the soma and dendrites. Furthermore, plastic changes in the expression of voltage-gated channels in the AIS have been shown to dynamically regulate neuronal excitability.

Site of Action Potential Initiation

Knowing where APs are generated within neurons is fundamental to an understanding of how synaptic inputs are converted

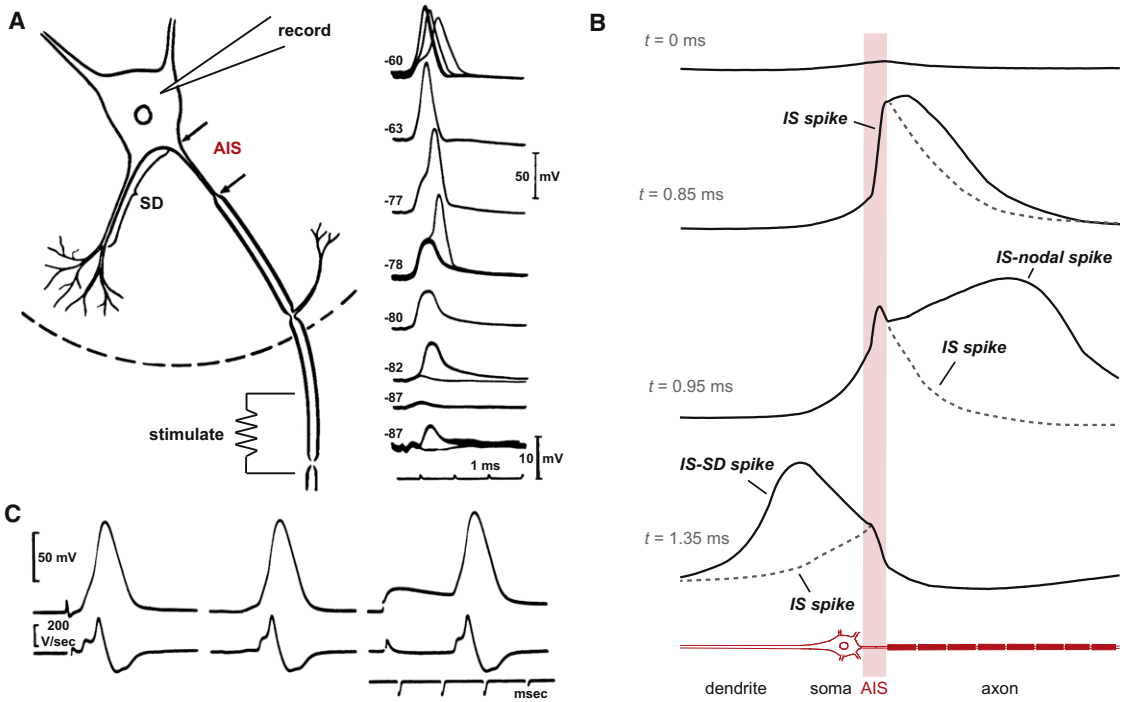

Figure 3. Action Potential Initiation in the Axon Initial Segment

(A) Left: schematic of the recording and stimulating situation. SD: somatodenritic; IS: initial segment. Right: antidromic action potentials (APs) recorded at the soma of a spinal motoneuron during hyperpolarization and depolarization to the indicated membrane potentials via somatic current injection. Adapted from Eccles (1955).

(B) Illustration of a voltage-space plot during AP initiation and propagation in a cortical pyramidal neuron model. Shown are voltage responses following somatic current injection (t = 0 ms) at the indicated times (left). AP initiation is characterized by rapid depolarization of the AIS (red transparent area; t = 0.85 ms) leading to generation of the IS spike, which first propagates down the axon to activate the first nodes of Ranvier (t = 0.95 ms). The IS spike then invades the somato-dendritic region initiating a SD spike, which backpropagates into the dendritic tree (t = 1.35 ms). Dotted lines (gray) indicate the voltage-space distribution in the absence of nodal Na^+ channels (t = 0.85 and 0.95 ms) or somato-dendritic Na^+ channels (t = 1.35 ms) to illustrate the IS spike in isolation. Adapted from Kole et al., 2008 (http://senselab.med.yale.edu/ModelDB/ShowModel.asp?model=114394).

(C) APs (top) and the differentiated AP waveform (bottom), evoked by antidromic stimulation (left), synaptic stimulation (middle), and somatic current injection (right) in a spinal motoneuron. Adapted from Fatt (1957).

into an output. Not surprisingly, this was one of the first questions tackled following the introduction of the method of intracellular recording, developed by Graham and Gerard (1946), to the CNS. The idea that APs are initiated in the AIS comes from a series of landmark experiments by a number of laboratories in the mid-1950s (Araki and Otani, 1955; Coombs et al., 1957; Fatt, 1957; Fuortes et al., 1957). Intracellular recordings from spinal motoneurons indicated that hyperpolarizing current injection via the somatic recording electrode progressively caused APs, evoked by activation of distal muscle nerves, to separate into different components (Figure 3A). These components were thought to originate from the soma and proximal dendrites (the so-called SD spike) and the axon initial segment (the so-called IS spike). The temporal relationship between the IS spike and how it propagates both orthodromically into the axon and antidromically into the soma, where it recruits somatic and dendritic Na^+ channels to generate the SD spike, is shown in Figure 3B. The different components underlying AP generation are more easily seen following differentiation of the somatic AP waveform. Importantly, these different components are observed irrespective of how APs are evoked (Figure 3C), leading to the conclusion that under physiological conditions (i.e., during synaptic input) APs are initiated in the AIS. Consistent with this idea, there is now direct experimental evidence from a number of different neuronal types that AP initiation in neurons of the CNS occurs at the distal part of the AIS, 20 to 40 μm from the soma (Atherton et al., 2008; Foust et al., 2010; Kole et al., 2007; Meeks and Mennerick, 2007; Palmer et al., 2010; Palmer and Stuart, 2006; Popovic et al., 2011; Schmidt-Hieber et al., 2008; Shu et al., 2007a).

What is the advantage of AP initiation in the AIS? The answer to this important question can be understood by comparing the properties of the AIS to neighboring structures. The AIS typically originates at or near the soma and so is ideally positioned to sample the synaptic inputs a neuron receives. Furthermore, the AIS has a small diameter—an order of magnitude smaller than that of the cell body. As such this compartment has a small local capacitance (C) and therefore requires less inward current (I), that is, a smaller number of Na^+ channels per unit area, to generate APs compared to larger structures, such as the soma or proximal dendrites. Hence, the AIS is also an energetically favorable site for AP initiation. Furthermore, the small capacitance of the AIS favors rapid changes in membrane potential, as occurs during the upstroke of the AP ($dV/dt = I/C$). Finally, it is worth noting that having a single site of AP generation provides neurons a single locus where inhibition can gate AP initiation.

AP Properties and Temporal Coding

One of the consequences of initiation of APs in the AIS, followed by backpropagation to the soma, is that from a somatic point of view the temporal relationship between synaptic input and AP initiation is distorted. As a result AP threshold is more depolarized at the soma than in the AIS (Kole and Stuart, 2008), and somatic AP threshold shows increased variability compared to that in the AIS (Yu et al., 2008). The geometry of the AIS (degree of taper and diameter), as well as the location, density, and properties of Na^+ channel in the AIS, influences the capacity of APs initiated in the AIS to propagate back to the soma (Hu et al., 2009; Mainen et al., 1995; Moore et al., 1983). It might be expected, therefore, that the location of Na^+ channels in AIS will influence somatic AP voltage threshold. Consistent with this, the location of Na^+ channels in the AIS is thought to underlie differences in somatic AP threshold between hippocampal dentate granule and CA3 pyramidal neurons (Kress et al., 2010).

The precise location and density of Na^+ channels in the AIS can also influence the fidelity of AP initiation. Initiation of APs further from the soma, taking advantage of the electrical isolation of this region, is a strategy used in some neurons to increase their capacity to discriminate the arrival time of different synaptic inputs. In neuronal pathways associated with hearing this helps determination of interaural timing differences (ITD). In nuclueus laminaris (NL) neurons in birds the distance of the AIS from the soma, as well as its length, depends on the characteristic frequency of presynaptic inputs the neuron receives (Kuba et al., 2006; Kuba and Ohmori, 2009). Na^+ channels in the AIS are located more distally from the soma in neurons that have high characteristic frequencies (>2 kHz) compared to neurons tuned to low characteristic frequencies ($\leq$1 kHz). Modeling indicates that the more distal location of the AIS in neurons that received inputs with high characteristic frequencies increases their capacity to detect ITDs. This occurred for two reasons. First, the passive cell body of NL neurons acts as a leak decreasing the membrane time constant and reducing the filtering of synaptic input frequencies (Ashida et al., 2007). Second, the distal position of Na^+ channels in the AIS reduces steady-state inactivation, increasing the number of Na^+ channels available for activation (Kuba et al., 2006). In separate experiments on relay neurons of the avian nucleus magnacellularis (NM), it was observed that the density of Na^+ channels in the AIS influences AP precision and is matched to the amplitude of the synaptic inputs a NM neuron receives (Kuba and Ohmori, 2009). NM neurons that receive a large number of small inputs had higher AIS Na^+ channel densities, improving AP precision, whereas NM neurons that receive a smaller number of large inputs had lower AIS Na^+ channel densites.

Voltage-gated K^+ channels in the AIS also play an important role in regulation AP firing. In pyramidal neurons K_v1 channels, generating D-type current, have been shown to delay the onset of AP firing in response to sustained depolarisation (Storm, 1988), as well as influence AP threshold and interspike interval (Bekkers and Delaney, 2001; Goldberg et al., 2008), whereas K_v7 channels influence spike-frequency adaptation, subthreshold resonance, and both spontaneous and AP burst firing (Hu et al., 2007; Peters et al., 2005; Shah et al., 2008; Yue and Yaari, 2004). K_v1 channels are the main K^+ channel involved in regulating AP half-width in the AIS and the axon proper (Figure 4A) (Kole et al., 2007; Shu et al., 2007b). With increasing distance from the soma the axonal AP half-width decreases steeply in parallel with an increase in the afterhyperpolarization (Kole et al., 2007). As a result, in cortical pyramidal neurons the AP half-width is ~250 μs at the distal end of the AIS, similar to that of APs recorded in axonal boutons (Alle and Geiger, 2006;

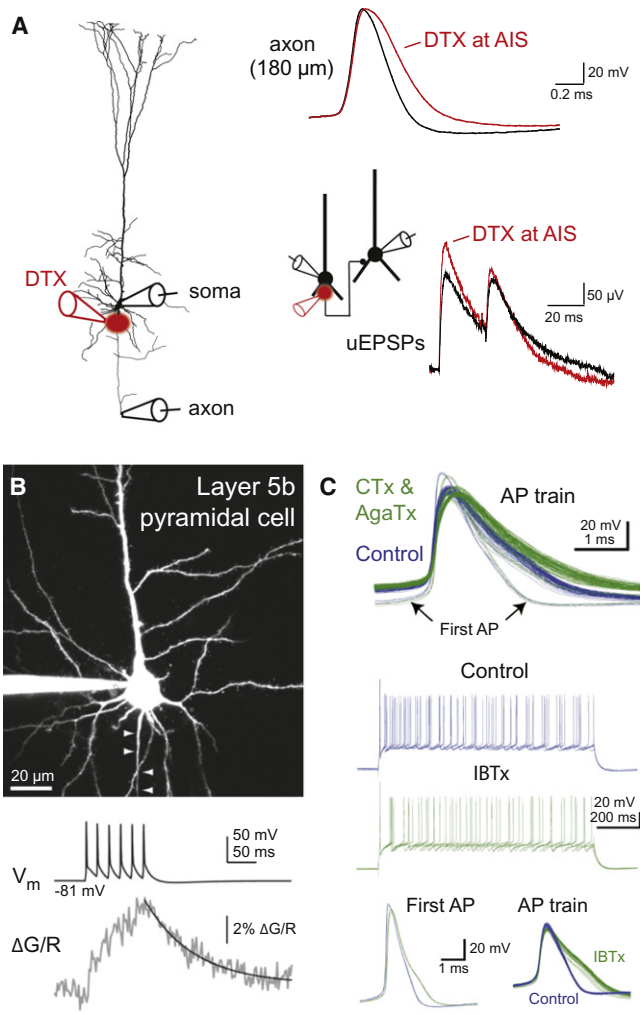

Figure 4. The AIS Regulates Axonal AP Duration and Transmitter Release

(A) Left: schematic of the experimental arrangement. Right: impact of local block of AIS K_v1 channels by dendrotoxin (DTX, red) on an axonal AP recorded 180 μm from the soma (top) and unitary EPSPs recorded from synaptically connected layer 5 pyramidal neurons (bottom). Adapted from Kole et al. (2007).

(B) Top: image of a layer 5 pyramidal neuron filled with a calcium-sensitive fluorescent dye. Bottom: examples of calcium transients (bottom) recorded from the AIS in response to a train of APs (top). Adapted from Bender and Trussell (2009).

(C) Top: axonal APs recorded in a layer 5 pyramidal neuron in control (blue) and during block of P/Q and N-type voltage-gated calcium channels by local application of ω-conotoxin (Ctx) and ω-agatoxin (AgaTx) to the AIS (green). Bottom: block of BK calcium-activated potassium channels in the AIS by iberiotoxin (IBTx) leads to an increase in axonal AP duration, similar to that seen during block of AIS P/Q and N-type voltage-gated calcium channels. Adapted from Yu et al. (2010).

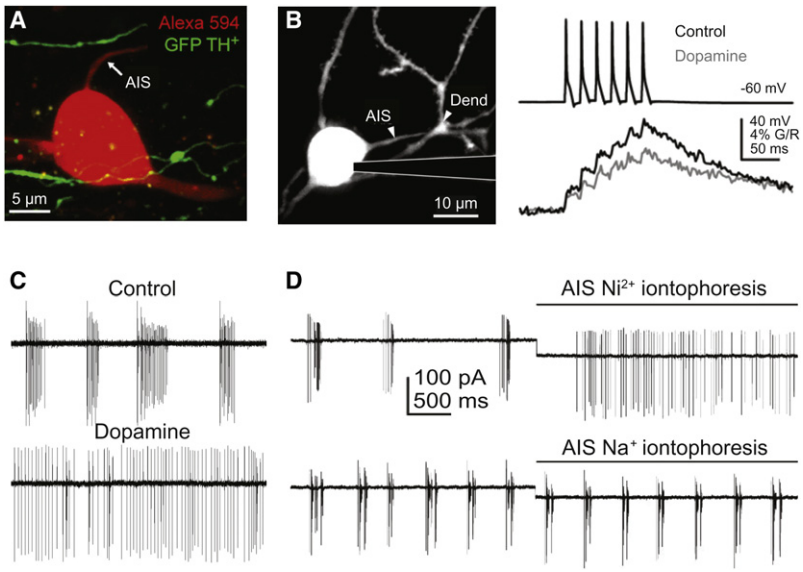

Figure 5. Dopamine Modulation of AIS Ca^{2+} Channels Regulates AP Firing

(A) Labeled cartwheel cell from the dorsal cochlear nucleus (red) in a slice from a mouse expressing GFP in dopamine-releasing axons containing tyrosine-hydroxylase (green). Adapted from Bender et al. (2010).

(B) Left: two-photon image of a cartwheel cell filled with a calcium-sensitive dye with the AIS and a dendrite indicated. Right: APs recorded at the soma (top) and associated Ca^{2+} transients (bottom) recorded from the AIS in control (black) and in the presence of dopamine (gray; 500 nM). Adapted from Bender et al. (2010).

(C) Cell-attached recordings of spontaneous AP firing in a cartwheel cell. Dopamine application reduces high-frequency burst firing.

(D) Single trials in which either the nonspecific T-type Ca^{2+} channel blocker Ni^{2+} or Na^{+} was iontophoresed onto the AIS. Scale applies to (C) and (D). Adapted from Bender et al., (2012).

Alle et al., 2009). Keeping the AP in the AIS brief is likely to be crucial for enabling rapid recovery of Na^{+} channels from inactivation, consistent with the absence of AP failures in the AIS even at high frequencies (Popovic et al., 2011). More recent work indicates that calcium influx through AIS voltage-gated Ca^{2+} channels (Figure 4B) can activate calcium-activated K^{+} channels in the AIS of pyramidal neurons in ferret prefrontal cortex (Figure 4C) (Yu et al., 2010), providing an additional means to regulate axonal AP repolarization. Whether this observation can be extended to the AIS of other neuronal cell types remains to be tested. Together, these data indicate that K^{+} channels in the AIS play a critical role in regulating axonal AP width and thereby the AP firing pattern in response to synaptic input.

Recent observations also indicate that ion channels in the AIS can be modulated by neurotransmitters, thereby influencing AP firing patterns. This has been investigated in glycinergic brain stem interneurons, called cartwheel cells, where T-type Ca^{2+} channels in the AIS are selectively inhibited by dopamine, via a protein kinase C pathway (Figures 5A and 5B) (Bender et al., 2010). As a result the mode of spontaneous AP firing is converted from high-frequency bursts to tonic firing (Figures 5C and 5D) (Bender et al., 2012). While dopamine acts in this system via volume transmission, its action is selective to the AIS, providing a powerful and efficient means to regulate AP firing. It will be of interest to see whether such selective AIS neuromodulation occurs in other neural cell types that show burst firing, and if so under which physiological conditions.

Role of the AIS in Synaptic Integration and Transmitter Release

Work over a decade ago indicated an important role of the somatic membrane potential in regulating transmitter release via axonal K^{+} channels (Debanne et al., 1997). More recent findings indicate that this can occur due to propagation of subthreshold changes in membrane potential significant distances down the axon of neurons, leading to modulation of transmitter release (Alle and Geiger, 2006; Shu et al., 2006). In cortical pyramidal neurons this occurs due to inactivation of K_v1 channels located in the AIS, which broadens of the axon AP waveform and increases unitary EPSP amplitude (Kole et al., 2007; Shu et al., 2007b). By regulating axonal AP half-width, AIS K_v1 channels can determine the duration of axonal APs and thereby transmitter release (Figure 4A) (Kole et al., 2007). This presumably occurs via regulation of Ca^{2+} influx into presynaptic terminals, which predominantly occurs during AP repolarization. Consistent with this, calcium chelators can partially block the capacity of subthreshold depolarizations to facilitate transmitter release (Alle and Geiger, 2006; Shu et al., 2006) (although see Scott et al., 2008). Furthermore, modulation of K_v1 channels, presumably located in the AIS, can influence spike-timing-dependent synaptic plasticity (Cudmore et al., 2010). Together, these observations show that the AIS is more than a simple on/off (binary) switch solely involved in AP generation. Rather, it can in addition act independently from the somato-dendritic region to regulate neuronal output in a graded analog fashion.

GABAergic Excitation and Inhibition

In addition to being critical for intrinsic excitability, the AIS of some neuronal types recieves synaptic input (see Figure 1). In cortical pyramidal neurons this input is exclusively GABA-ergic, and from a specific set of interneurons called chandelier or axo-axonic cells (Somogyi et al., 1998). These terminals are found in the neocortex and hippocampus, where they align to postsynaptic GABA receptors containing $\alpha 2$ subunits, and are thought to provide inhibitory control over AP initiation (Howard et al., 2005; Nusser et al., 1996; Zhu et al., 2004). While these GABAergic inputs are in a prime position to inhibit AP potential output, recent evidence suggests they may play both an inhibitory and an excitatory role (Figures 6A–6C) (Woodruff et al., 2010). In both the cortex and amygdala activation of axo-axonic cells can under some circumstances excite surrounding pyramidal neurons (Szabadics et al., 2006; Woodruff et al., 2006). This has been proposed to occur as a result of a high intracellular chloride concentration in the AIS due to the low expression of the KCC2 chloride transporter, which pumps chloride out of neurons (Figure 6A) (Szabadics et al., 2006). Consistent with this, recent work using uncaging of GABA to different regions

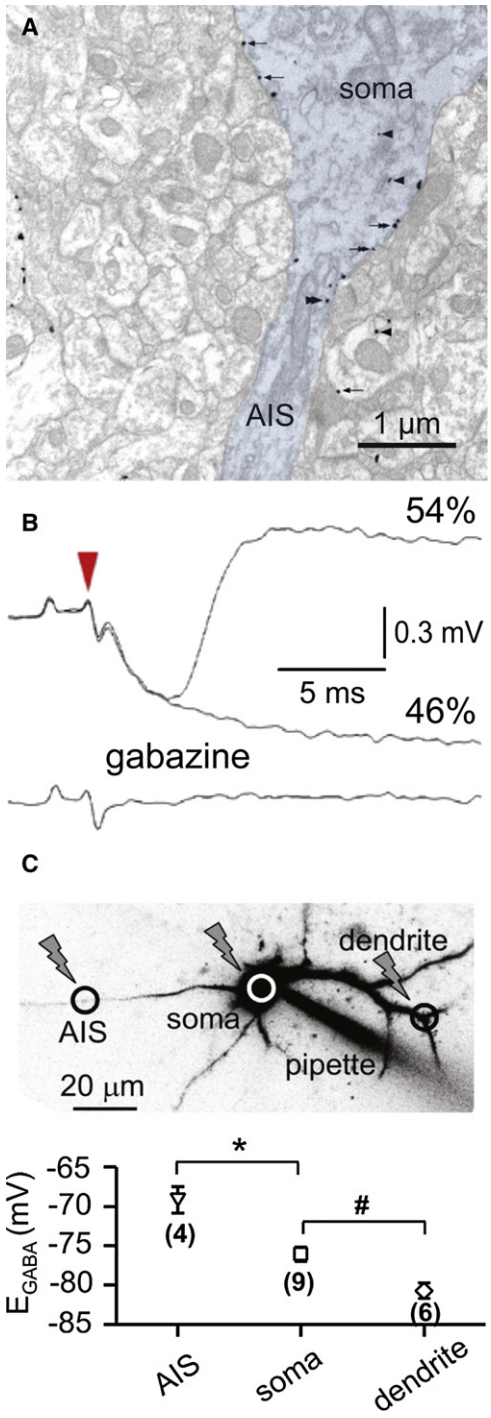

Figure 6. Excitatory GABAergic Inputs to the Axon Initial Segment

(A) Electron micrograph showing that expression of the KCC2 chloride transporter (dark spots) is present at the axon hillock and soma but absent from of the axon initial segment (AIS) of a cortical pyramidal neuron. Adapted from Szabadics et al. (2006).

(B) APs in an axo-axonic interneuron (red arrow) evoke pure monosynaptic IPSPs on 46% of trials, and IPSPs followed by disynaptic EPSPs in 54% of trials, in a cortical pyramidal neuron. Application of the $GABA_A$ antagonist gabazine (20 μM) abolished both IPSPs and EPSPs, indicating an excitatory action of axo-axonic interneurons. Adapted from Szabadics et al. (2006).

(C) Top: schematic of the experimental recording situation during uncaging of GABA on to AIS, soma, and dendrites of a layer 2/3 pyramidal neuron. Bottom: summary data on the reversal potential for GABA (E_{GABA}) in different neuronal compartments. Note that E_{GABA} is more depolarized in the AIS. Adapted from Khirug et al. (2008).

of pyramidal neurons indicates that the reversal potential for GABA in the AIS is depolarized compared to that at the soma or in the dendrites (Figure 6C) (Khirug et al., 2008). How axo-axonic inputs at the AIS enhance AP output, and in particular under which physiological conditions this occurs, requires further investigation.

Activity-Dependent Plasticity and Homeostatic Regulation

One of the more remarkable discoveries on AIS function in recent years is that despite the highly organized control of ion channels in the AIS membrane the location and density of these channels is not fixed. Two studies indicated that Na^+ channels in the AIS can translocate and undergo changes in position in response to changes in electrical activity (Grubb and Burrone, 2010a; Kuba et al., 2010). A loss in presynaptic input to chick NL neurons leads to an increase in the length of the AIS expressing Na^+ channels and associated proteins (Kuba et al., 2010), whereas chronic increases in AP firing in cultured hippocampal neurons causes a shift of the region of the AIS expressing Na^+ channels to more distal locations (Grubb and Burrone, 2010a). Both AIS modifications spanned considerable distances (~10 to 20 μm), are long lasting, bidirectional, and importantly correlated with changes in intrinsic excitability. These findings suggest that activity-dependent regulation of AIS proteins is an important mechanism for maintaining homeostasis of intrinsic excitability. The precise molecular mechanisms involved are not well understood but have been shown to involve L-type Ca^{2+} channels and calcium-dependent modification of cytoskeletal proteins such as Ankyrin G (Grubb and Burrone, 2010a). Importantly, L-type Ca^{2+} channels have so far not been observed at the AIS, indicating that the source of calcium underlying plasticity in the AIS arises from a different location. The binding of Na^+ channels to Ankyrin G in the AIS can be facilitated by phosphorylation of casein kinase II, a protein enriched in the AIS and nodes of Ranvier (Bréchet et al., 2008), which may provide a mechanism for plastic changes in Na^+ channel expression in the AIS. Of great importance will be to determine whether similar activity-dependent AIS plasticity can occur in the adult CNS.

The AIS and Disease

Given the fact that even small changes in the AIS can generate profound changes in excitability it may not be surprising that mutations in AIS proteins, due to failure in protein expression or trafficking, may contribute to pathogenesis of neurological disorders. One of the earliest indications of a possible role of the AIS in epilepsy came from anatomical observations that GABA-ergic synapses targeting the AIS of cortical pyramidal neurons are lost in the epileptic foci (Ribak, 1985). While on average the AIS of pyramidal neurons receives input from only five axo-axonic cells, each axo-axonic cell projects to ~250 different cortical or ~1,000 hippocampal neurons, placing these cells in a strategic position to synchronize large neural networks.

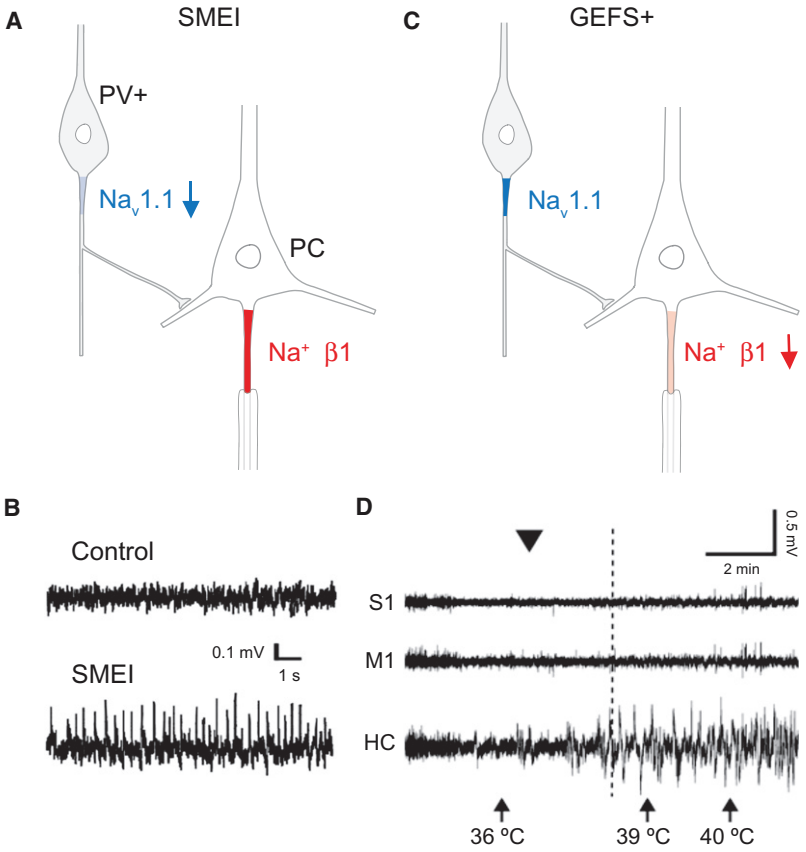

Figure 7. The Axon Initial Segment and Epilepsy

(A) Schematic showing that severe myoclonic epilepsy in infancy (SMEI) is associated with loss-of-function of $Na_v1.1$ channels located in the AIS of parvalbumin positive (PV+) interneurons.

(B) An animal model of SMEI (bottom) shows spontaneous seizures (recorded via ictal ECoG) compared to control littermates (top). Adapted from Ogiwara et al. (2007).

(C) Patients with genetic epilepsy with febrile seizures plus (GEFS+) carry a mutation in the Na^+ channel β1 subunit (C121W), leading to a loss of β1 selectively from the AIS of pyramidal cells (PC).

(D) Example of a mouse heterozygous for the C121W mutation showing a febrile seizure phenotype. ECoGs from somatosensory (S1), motor cortex (M1), and hippocampus (HC). Increasing core temperature (arrowhead; temperatures indicated at the bottom) leads to epileptiform activity. Dashed vertical line represents start of behavioral arrest phenotype, which occurred at 38.5°C. The first signs of epileptic activity were seen in the hippocampus. Adapted from Wimmer et al. (2010a).

This synchronizing action of axo-axonic cells agrees well with an important role of the focal loss of these cells in temporal lobe epilepsy and has led to the hypothesis that loss of inhibition at the AIS contributes to the etiology of epilepsy (DeFelipe, 1999). Deficits in axo-axonic cell function have also been detected in subjects with schizophrenia (Lewis, 2011). As described above, recent work indicates that axo-axonic cells can also be excitatory. Consistent with this, in vitro models of seizures indicate that axo-axonic cells are involved in the generation of a positive feedback circuit during epileptic events (Fujiwara-Tsukamoto et al., 2004). It remains to be established whether the loss of axo-axonic cells in epilepsy, or deficits in axo-axonic cell function in schizophrenia, play a causal role in disease pathogenesis or result as a consequence of it.

AIS Channelopathies and the Pathogenesis of Epilepsy

More direct evidence of a causal role of the AIS in neurological disorders comes from recent studies focusing on inherited epilepsy syndromes (Wimmer et al., 2010b). From the hundreds of epilepsy-associated mutations in ion channels, many are known to cluster at the AIS. For example, the Na^+ channel isoform $Na_v1.1$ is predominantly expressed in the AIS and distal axon of parvalbumin (PV)-positive interneurons in the cortex and hippocampus, as well as in Purkinje neuron axons (Lorincz and Nusser, 2008; Ogiwara et al., 2007). Recently, Ogiwara et al. (2007) generated knockin mice carrying a loss-of-function mutation in $Na_v1.1$ (*SCN1A* gene), which in humans is associated with severe myoclonic epilepsy in infancy. Recordings from PV-positive interneurons in $Na_v1.1$ knockout mice showed increased spike frequency adaptation, consistent with reduced somatic whole-cell Na^+ current (Ogiwara et al., 2007; Yu et al., 2006). As expected from a loss in inhibitory drive these mice showed epileptic spontaneous seizures (Figures 7A and 7B). Similarly, a mutation in the *SCN1B* gene coding for the Na^+ channel β1 subunit (C121W) can lead to generalized epilepsy with febrile seizures in humans. Mice heterozygous for the C121W mutation lack the high density of the β1 subunit found in the AIS of normal mice (Wimmer et al., 2010a). Electrophysiological recordings in pyramidal neurons from mice carrying the mutation showed an increase in AP number during high-frequency bursts and a lower threshold for temperature-dependent seizure generation (Figures 7C and 7D) (Wimmer et al., 2010a), consistent with the epileptic phenotype in humans. Other major epilepsy mutations include loss-of-function mutations in $K_v7.2/7.3$ channels, causing benign familial neonatal convulsions (Biervert et al., 1998; Castaldo et al., 2002). Although $Na_v1.1$, the Na^+ channel β1 subunit, and $K_v7.2/7.3$ are all major components of the AIS, these channels are also expressed in other axonal domains, including nodes of Ranvier and presynaptic terminals, or at low densities in the soma and dendrites (Debanne et al., 2011). Whether the epilepsies described above are exclusively due to changes in the AIS or are also dependent on ion channel modifications at other locations is currently not clear.

Although none of the above studies has demonstrated that changes in the AIS alone are sufficient to cause disease, a genetic variation in the gene coding for contactin-associated protein 2 (Caspr-2), which is exclusively expressed in AIS and nodes of Ranvier, is associated with abnormalities in brain development and focal epilepsies (Strauss et al., 2006). Further support for the AIS in disease comes from recent molecular work showing that other cytoskeletal proteins expressed in the

AIS and nodes of Ranvier are also vulnerable to neurological insults. Schafer et al. (2009) using in vivo and in vitro models of ischemia in mice observed large increases in the cysteine protease calpain in the AIS. Calpain, a Ca^{2+} dependent protease, was found to cause direct proteolysis of Ankyrin G and βIV spectrin, leading to disruption of the AIS protein assembly and a reduction in AIS Na^{+} channel density (Schafer et al., 2009). Interestingly, despite an overlap in the molecular structure of the AIS and nodes of Ranvier, the loss of βIV spectrin was not observed in nodes of Ranvier, suggesting that the injury target during ischemia is the AIS. Although voltage-gated Ca^{2+} channel expression has been found at the AIS of central neurons (Bender and Trussell, 2009; Yu et al., 2010), the Ca^{2+} source for structural plasticity at the AIS seems to derive from L-type Ca^{2+} channels, which are expressed at the cell body (Grubb and Burrone, 2010a). How activity, Ca^{2+} elevations, and AIS structural proteins interact is likely to be a major target for further investigations and will have major implications for our understanding of how the AIS responds to both physiological and pathological activity. In conclusion, these studies suggest that mutations in ion channels and associated proteins expressed in the AIS, in both inhibitory and excitatory neurons, may play a critical role in the pathogenesis of epileptic syndromes and stroke and warrant further investigation in other diseases (Buffington and Rasband, 2011).

Conclusion and Outlook

Mounting evidence has emerged over the last decade indicating that the AIS, traditionally viewed solely as a trigger zone for AP generation, plays a central role in tuning and regulating intrinsic neuronal excitability as well as transmitter release. Rapidly expanding technical possibilities make the AIS now accessible to physiological manipulation and recording. For example, it is now possible to target channelrhodopsin 2 to the AIS (Grubb and Burrone, 2010b) or to monitor voltage signals in small axonal segments with high resolution using voltage-sensitive dyes (Popovic et al., 2011). Together with advances in molecular and genetic tools, future research is expected to increase our knowledge of AIS function. We will need to answer questions such as: Under which physiological and pathological conditions do changes in the AIS occur? Can these changes also occur in the adult system? And what are the basic molecular mechanisms underlying this plasticity? We predict that the coming years will reveal additional complex operations associated with AIS function. Such information will not only provide fundamental insights into how the AIS affects AP generation and information processing in neurons, but may also open new avenues for targeted therapies to treat neurological disorders.

REFERENCES

Alle, H., and Geiger, J.R. (2006). Combined analog and action potential coding in hippocampal mossy fibers. Science *311*, 1290–1293.

Alle, H., Roth, A., and Geiger, J.R.P. (2009). Energy-efficient action potentials in hippocampal mossy fibers. Science *325*, 1405–1408.

Araki, T., and Otani, T. (1955). Response of single motoneurons to direct stimulation in toad's spinal cord. J. Neurophysiol. *18*, 472–485.

Ashida, G., Abe, K., Funabiki, K., and Konishi, M. (2007). Passive soma facilitates submillisecond coincidence detection in the owl's auditory system. J. Neurophysiol. *97*, 2267–2282.

Astman, N., Gutnick, M.J., and Fleidervish, I.A. (2006). Persistent sodium current in layer 5 neocortical neurons is primarily generated in the proximal axon. J. Neurosci. *26*, 3465–3473.

Atherton, J.F., Wokosin, D.L., Ramanathan, S., and Bevan, M.D. (2008). Autonomous initiation and propagation of action potentials in neurons of the subthalamic nucleus. J. Physiol. *586*, 5679–5700.

Azouz, R., Jensen, M.S., and Yaari, Y. (1996). Ionic basis of spike after-depolarization and burst generation in adult rat hippocampal CA1 pyramidal cells. J. Physiol. *492*, 211–223.

Bas Orth, C., Schultz, C., Müller, C.M., Frotscher, M., and Deller, T. (2007). Loss of the cisternal organelle in the axon initial segment of cortical neurons in synaptopodin-deficient mice. J. Comp. Neurol. *504*, 441–449.

Bekkers, J.M., and Delaney, A.J. (2001). Modulation of excitability by alpha-dendrotoxin-sensitive potassium channels in neocortical pyramidal neurons. J. Neurosci. *21*, 6553–6560.

Bender, K.J., and Trussell, L.O. (2009). Axon initial segment Ca2+ channels influence action potential generation and timing. Neuron *61*, 259–271.

Bender, K.J., Ford, C.P., and Trussell, L.O. (2010). Dopaminergic modulation of axon initial segment calcium channels regulates action potential initiation. Neuron *68*, 500–511.

Bender, K.J., Uebele, V.N., Renger, J.J., and Trussell, L.O. (2012). Control of firing patterns through modulation of axon initial segment T-type calcium channels. J. Physiol. *590*, 109–118.

Biervert, C., Schroeder, B.C., Kubisch, C., Berkovic, S.F., Propping, P., Jentsch, T.J., and Steinlein, O.K. (1998). A potassium channel mutation in neonatal human epilepsy. Science *279*, 403–406.

Boiko, T., Van Wart, A., Caldwell, J.H., Levinson, S.R., Trimmer, J.S., and Matthews, G. (2003). Functional specialization of the axon initial segment by isoform-specific sodium channel targeting. J. Neurosci. *23*, 2306–2313.

Bréchet, A., Fache, M.-P., Brachet, A., Ferracci, G., Baude, A., Irondelle, M., Pereira, S., Leterrier, C., and Dargent, B. (2008). Protein kinase CK2 contributes to the organization of sodium channels in axonal membranes by regulating their interactions with ankyrin G. J. Cell Biol. *183*, 1101–1114.

Brown, D.A., and Passmore, G.M. (2009). Neural KCNQ (Kv7) channels. Br. J. Pharmacol. *156*, 1185–1195.

Buffington, S.A., and Rasband, M.N. (2011). The axon initial segment in nervous system disease and injury. Eur. J. Neurosci. *34*, 1609–1619.

Calabrese, R.L., and Kennedy, D. (1974). Multiple sites of spike initiation in a single dendritic system. Brain Res. *82*, 316–321.

Callewaert, G., Eilers, J., and Konnerth, A. (1996). Axonal calcium entry during fast 'sodium' action potentials in rat cerebellar Purkinje neurones. J. Physiol. *495*, 641–647.

Castaldo, P., del Giudice, E.M., Coppola, G., Pascotto, A., Annunziato, L., and Taglialatela, M. (2002). Benign familial neonatal convulsions caused by altered gating of KCNQ2/KCNQ3 potassium channels. J. Neurosci. *22*, RC199.

Castelli, L., Biella, G., Toselli, M., and Magistretti, J. (2007). Resurgent Na+ current in pyramidal neurones of rat perirhinal cortex: axonal location of channels and contribution to depolarizing drive during repetitive firing. J. Physiol. *582*, 1179–1193.

Catterall, W.A. (1981). Localization of sodium channels in cultured neural cells. J. Neurosci. *1*, 777–783.

Colbert, C.M., and Johnston, D. (1996). Axonal action-potential initiation and Na+ channel densities in the soma and axon initial segment of subicular pyramidal neurons. J. Neurosci. *16*, 6676–6686.

Colbert, C.M., and Pan, E. (2002). Ion channel properties underlying axonal action potential initiation in pyramidal neurons. Nat. Neurosci. *5*, 533–538.

Coombs, J.S., Curtis, D.R., and Eccles, J.C. (1957). The interpretation of spike potentials of motoneurones. J. Physiol. *139*, 198–231.

Cudmore, R.H., Fronzaroli-Molinieres, L., Giraud, P., and Debanne, D. (2010). Spike-time precision and network synchrony are controlled by the homeostatic regulation of the D-type potassium current. J. Neurosci. *30*, 12885–12895.

Debanne, D., Guérineau, N.C., Gähwiler, B.H., and Thompson, S.M. (1997). Action-potential propagation gated by an axonal I(A)-like K+ conductance in hippocampus. Nature *389*, 286–289.

Debanne, D., Campanac, E., Bialowas, A., Carlier, E., and Alcaraz, G. (2011). Axon physiology. Physiol. Rev. *91*, 555–602.

DeFelipe, J. (1999). Chandelier cells and epilepsy. Brain *122*, 1807–1822.

Devaux, J.J., Kleopa, K.A., Cooper, E.C., and Scherer, S.S. (2004). KCNQ2 is a nodal K+ channel. J. Neurosci. *24*, 1236–1244.

Dodge, F.A., and Cooley, J.W. (1973). Action potential of the motoneuron. IBM J. Res. Develop. *17*, 219–229.

Dodson, P.D., Barker, M.C., and Forsythe, I.D. (2002). Two heteromeric Kv1 potassium channels differentially regulate action potential firing. J. Neurosci. *22*, 6953–6961.

Duflocq, A., Le Bras, B., Bullier, E., Couraud, F., and Davenne, M. (2008). Nav1.1 is predominantly expressed in nodes of Ranvier and axon initial segments. Mol. Cell. Neurosci. *39*, 180–192.

Eccles, J.C. (1955). The central action of antidromic impulses in motor nerve fibres. Pflugers Arch. *260*, 385–415.

Fatt, P. (1957). Sequence of events in synaptic activation of a motoneurone. J. Neurophysiol. *20*, 61–80.

Fleidervish, I.A., Lasser-Ross, N., Gutnick, M.J., and Ross, W.N. (2010). Na+ imaging reveals little difference in action potential-evoked Na+ influx between axon and soma. Nat. Neurosci. *13*, 852–860.

Foust, A., Popovic, M., Zecevic, D., and McCormick, D.A. (2010). Action potentials initiate in the axon initial segment and propagate through axon collaterals reliably in cerebellar Purkinje neurons. J. Neurosci. *30*, 6891–6902.

Fujiwara-Tsukamoto, Y., Isomura, Y., Kaneda, K., and Takada, M. (2004). Synaptic interactions between pyramidal cells and interneurone subtypes during seizure-like activity in the rat hippocampus. J. Physiol. *557*, 961–979.

Fuortes, M.G., Frank, K., and Becker, M.C. (1957). Steps in the production of motoneuron spikes. J. Gen. Physiol. *40*, 735–752.

Garrido, J.J., Giraud, P., Carlier, E., Fernandes, F., Moussif, A., Fache, M.-P., Debanne, D., and Dargent, B. (2003). A targeting motif involved in sodium channel clustering at the axonal initial segment. Science *300*, 2091–2094.

Goldberg, E.M., Clark, B.D., Zagha, E., Nahmani, M., Erisir, A., and Rudy, B. (2008). K+ channels at the axon initial segment dampen near-threshold excitability of neocortical fast-spiking GABAergic interneurons. Neuron *58*, 387–400.

Graham, J., and Gerard, R.W. (1946). Membrane potentials and excitation of impaled single muscle fibers. J. Cell. Physiol. *28*, 99–117.

Grubb, M.S., and Burrone, J. (2010a). Activity-dependent relocation of the axon initial segment fine-tunes neuronal excitability. Nature *465*, 1070–1074.

Grubb, M.S., and Burrone, J. (2010b). Channelrhodopsin-2 localised to the axon initial segment. PLoS ONE *5*, e13761.

Hartline, D.K., and Colman, D.R. (2007). Rapid conduction and the evolution of giant axons and myelinated fibers. Curr. Biol. *17*, R29–R35.

Hill, A.S., Nishino, A., Nakajo, K., Zhang, G., Fineman, J.R., Selzer, M.E., Okamura, Y., and Cooper, E.C. (2008). Ion channel clustering at the axon initial segment and node of Ranvier evolved sequentially in early chordates. PLoS Genet. *4*, e1000317.

Hodgkin, A.L., and Huxley, A.F. (1952). A quantitative description of membrane current and its application to conduction and excitation in nerve. J. Physiol. *117*, 500–544.

Howard, A., Tamas, G., and Soltesz, I. (2005). Lighting the chandelier: new vistas for axo-axonic cells. Trends Neurosci. *28*, 310–316.

Hu, H., Vervaeke, K., and Storm, J.F. (2007). M-channels (Kv7/KCNQ channels) that regulate synaptic integration, excitability, and spike pattern of CA1 pyramidal cells are located in the perisomatic region. J. Neurosci. *27*, 1853–1867.

Hu, W., Tian, C., Li, T., Yang, M., Hou, H., and Shu, Y. (2009). Distinct contributions of Na(v)1.6 and Na(v)1.2 in action potential initiation and backpropagation. Nat. Neurosci. *12*, 996–1002.

Inda, M.C., DeFelipe, J., and Muñoz, A. (2006). Voltage-gated ion channels in the axon initial segment of human cortical pyramidal cells and their relationship with chandelier cells. Proc. Natl. Acad. Sci. USA *103*, 2920–2925.

Jarnot, M.D., and Corbett, A.M. (1995). High titer antibody to mammalian neuronal sodium channels produces sustained channel block. Brain Res. *674*, 159–162.

Johnston, J., Griffin, S.J., Baker, C., Skrzypiec, A., Chernova, T., and Forsythe, I.D. (2008). Initial segment Kv2.2 channels mediate a slow delayed rectifier and maintain high frequency action potential firing in medial nucleus of the trapezoid body neurons. J. Physiol. *586*, 3493–3509.

Khirug, S., Yamada, J., Afzalov, R., Voipio, J., Khiroug, L., and Kaila, K. (2008). GABAergic depolarization of the axon initial segment in cortical principal neurons is caused by the Na-K-2Cl cotransporter NKCC1. J. Neurosci. *28*, 4635–4639.

Klinger, F., Gould, G., Boehm, S., and Shapiro, M.S. (2011). Distribution of M-channel subunits KCNQ2 and KCNQ3 in rat hippocampus. Neuroimage *58*, 761–769.

Kole, M.H. (2011). First node of Ranvier facilitates high-frequency burst encoding. Neuron *71*, 671–682.

Kole, M.H.P., and Stuart, G.J. (2008). Is action potential threshold lowest in the axon? Nat. Neurosci. *11*, 1253–1255.

Kole, M.H.P., Letzkus, J.J., and Stuart, G.J. (2007). Axon initial segment Kv1 channels control axonal action potential waveform and synaptic efficacy. Neuron *55*, 633–647.

Kole, M.H.P., Ilschner, S.U., Kampa, B.M., Williams, S.R., Ruben, P.C., and Stuart, G.J. (2008). Action potential generation requires a high sodium channel density in the axon initial segment. Nat. Neurosci. *11*, 178–186.

Kordeli, E., Lambert, S., and Bennett, V. (1995). AnkyrinG. A new ankyrin gene with neural-specific isoforms localized at the axonal initial segment and node of Ranvier. J. Biol. Chem. *270*, 2352–2359.

Kress, G.J., Dowling, M.J., Eisenman, L.N., and Mennerick, S. (2010). Axonal sodium channel distribution shapes the depolarized action potential threshold of dentate granule neurons. Hippocampus *20*, 558–571.

Kuba, H., and Ohmori, H. (2009). Roles of axonal sodium channels in precise auditory time coding at nucleus magnocellularis of the chick. J. Physiol. *587*, 87–100.

Kuba, H., Ishii, T.M., and Ohmori, H. (2006). Axonal site of spike initiation enhances auditory coincidence detection. Nature *444*, 1069–1072.

Kuba, H., Oichi, Y., and Ohmori, H. (2010). Presynaptic activity regulates Na(+) channel distribution at the axon initial segment. Nature *465*, 1075–1078.

Lewis, D.A. (2011). The chandelier neuron in schizophrenia. Dev. Neurobiol. *71*, 118–127.

Lorincz, A., and Nusser, Z. (2008). Cell-type-dependent molecular composition of the axon initial segment. J. Neurosci. *28*, 14329–14340.

Lorincz, A., and Nusser, Z. (2010). Molecular identity of dendritic voltage-gated sodium channels. Science *328*, 906–909.

Magee, J.C., and Johnston, D. (1995). Characterization of single voltage-gated Na+ and Ca2+ channels in apical dendrites of rat CA1 pyramidal neurons. J. Physiol. *487*, 67–90.

Mainen, Z.F., Joerges, J., Huguenard, J.R., and Sejnowski, T.J. (1995). A model of spike initiation in neocortical pyramidal neurons. Neuron *15*, 1427–1439.

Maratou, E., and Theophilidis, G. (2000). An axon pacemaker: diversity in the mechanism of generation and conduction of action potentials in snail neurons. Neuroscience *96*, 1–2.

Meeks, J.P., and Mennerick, S. (2007). Action potential initiation and propagation in CA3 pyramidal axons. J. Neurophysiol. *97*, 3460–3472.

Meyrand, P., Weimann, J.M., and Marder, E. (1992). Multiple axonal spike initiation zones in a motor neuron: serotonin activation. J. Neurosci. *12*, 2803–2812.

Moore, J.W., Stockbridge, N., and Westerfield, M. (1983). On the site of impulse initiation in a neurone. J. Physiol. *336*, 301–311.

Nusser, Z., Sieghart, W., Benke, D., Fritschy, J.M., and Somogyi, P. (1996). Differential synaptic localization of two major gamma-aminobutyric acid type A receptor alpha subunits on hippocampal pyramidal cells. Proc. Natl. Acad. Sci. USA *93*, 11939–11944.

Ogawa, Y., Horresh, I., Trimmer, J.S., Bredt, D.S., Peles, E., and Rasband, M.N. (2008). Postsynaptic density-93 clusters Kv1 channels at axon initial segments independently of Caspr2. J. Neurosci. *28*, 5731–5739.

Ogiwara, I., Miyamoto, H., Morita, N., Atapour, N., Mazaki, E., Inoue, I., Takeuchi, T., Itohara, S., Yanagawa, Y., Obata, K., et al. (2007). Nav1.1 localizes to axons of parvalbumin-positive inhibitory interneurons: a circuit basis for epileptic seizures in mice carrying an Scn1a gene mutation. J. Neurosci. *27*, 5903–5914.

Palay, S.L., Sotelo, C., Peters, A., and Orkand, P.M. (1968). The axon hillock and the initial segment. J. Cell Biol. *38*, 193–201.

Palmer, L.M., and Stuart, G.J. (2006). Site of action potential initiation in layer 5 pyramidal neurons. J. Neurosci. *26*, 1854–1863.

Palmer, L.M., Clark, B.A., Gründemann, J., Roth, A., Stuart, G.J., and Häusser, M. (2010). Initiation of simple and complex spikes in cerebellar Purkinje cells. J. Physiol. *588*, 1709–1717.

Pan, Z., Kao, T., Horvath, Z., Lemos, J., Sul, J.-Y., Cranstoun, S.D., Bennett, V., Scherer, S.S., and Cooper, E.C. (2006). A common ankyrin-G-based mechanism retains KCNQ and NaV channels at electrically active domains of the axon. J. Neurosci. *26*, 2599–2613.

Peters, A., Proskauer, C.C., and Kaiserman-Abramof, I.R. (1968). The small pyramidal neuron of the rat cerebral cortex. The axon hillock and initial segment. J. Cell Biol. *39*, 604–619.

Peters, H.C., Hu, H., Pongs, O., Storm, J.F., and Isbrandt, D. (2005). Conditional transgenic suppression of M channels in mouse brain reveals functions in neuronal excitability, resonance and behavior. Nat. Neurosci. *8*, 51–60.

Popovic, M.A., Foust, A.J., McCormick, D.A., and Zecevic, D. (2011). The spatio-temporal characteristics of action potential initiation in layer 5 pyramidal neurons: a voltage imaging study. J. Physiol. *589*, 4167–4187.

Rasband, M.N. (2010). The axon initial segment and the maintenance of neuronal polarity. Nat. Rev. Neurosci. *11*, 552–562.

Ribak, C.E. (1985). Axon terminals of GABAergic chandelier cells are lost at epileptic foci. Brain Res. *326*, 251–260.

Royeck, M., Horstmann, M.-T., Remy, S., Reitze, M., Yaari, Y., and Beck, H. (2008). Role of axonal NaV1.6 sodium channels in action potential initiation of CA1 pyramidal neurons. J. Neurophysiol. *100*, 2361–2380.

Rush, A.M., Dib-Hajj, S.D., and Waxman, S.G. (2005). Electrophysiological properties of two axonal sodium channels, Nav1.2 and Nav1.6, expressed in mouse spinal sensory neurones. J. Physiol. *564*, 803–815.

Schafer, D.P., Jha, S., Liu, F., Akella, T., McCullough, L.D., and Rasband, M.N. (2009). Disruption of the axon initial segment cytoskeleton is a new mechanism for neuronal injury. J. Neurosci. *29*, 13242–13254.

Schmidt-Hieber, C., and Bischofberger, J. (2010). Fast sodium channel gating supports localized and efficient axonal action potential initiation. J. Neurosci. *30*, 10233–10242.

Schmidt-Hieber, C., Jonas, P., and Bischofberger, J. (2008). Action potential initiation and propagation in hippocampal mossy fibre axons. J. Physiol. *586*, 1849–1857.

Scott, R., Ruiz, A., Henneberger, C., Kullmann, D.M., and Rusakov, D.A. (2008). Analog modulation of mossy fiber transmission is uncoupled from changes in presynaptic Ca2+. J. Neurosci. *28*, 7765–7773.

Shah, M.M., Migliore, M., Valencia, I., Cooper, E.C., and Brown, D.A. (2008). Functional significance of axonal Kv7 channels in hippocampal pyramidal neurons. Proc. Natl. Acad. Sci. USA *105*, 7869–7874.

Shu, Y., Hasenstaub, A., Duque, A., Yu, Y., and McCormick, D.A. (2006). Modulation of intracortical synaptic potentials by presynaptic somatic membrane potential. Nature *441*, 761–765.

Shu, Y., Duque, A., Yu, Y., Haider, B., and McCormick, D.A. (2007a). Properties of action-potential initiation in neocortical pyramidal cells: evidence from whole cell axon recordings. J. Neurophysiol. *97*, 746–760.

Shu, Y., Yu, Y., Yang, J., and McCormick, D.A. (2007b). Selective control of cortical axonal spikes by a slowly inactivating K+ current. Proc. Natl. Acad. Sci. USA *104*, 11453–11458.

Somogyi, P., Tamás, G., Lujan, R., and Buhl, E.H. (1998). Salient features of synaptic organisation in the cerebral cortex. Brain Res. Brain Res. Rev. *26*, 113–135.

Storm, J.F. (1988). Temporal integration by a slowly inactivating K+ current in hippocampal neurons. Nature *336*, 379–381.

Strauss, K.A., Puffenberger, E.G., Huentelman, M.J., Gottlieb, S., Dobrin, S.E., Parod, J.M., Stephan, D.A., and Morton, D.H. (2006). Recessive symptomatic focal epilepsy and mutant contactin-associated protein-like 2. N. Engl. J. Med. *354*, 1370–1377.

Stuart, G.J., and Sakmann, B. (1994). Active propagation of somatic action potentials into neocortical pyramidal cell dendrites. Nature *367*, 69–72.

Stuart, G., and Sakmann, B. (1995). Amplification of EPSPs by axosomatic sodium channels in neocortical pyramidal neurons. Neuron *15*, 1065–1076.

Szabadics, J., Varga, C., Molnár, G., Oláh, S., Barzó, P., and Tamás, G. (2006). Excitatory effect of GABAergic axo-axonic cells in cortical microcircuits. Science *311*, 233–235.

Taddese, A., and Bean, B.P. (2002). Subthreshold sodium current from rapidly inactivating sodium channels drives spontaneous firing of tuberomammillary neurons. Neuron *33*, 587–600.

Tauc, L. (1962). Site of origin and propagation in spike in the giant neuron of Aplysia. J. Gen. Physiol. *45*, 1077–1097.

Van Wart, A., Trimmer, J.S., and Matthews, G. (2007). Polarized distribution of ion channels within microdomains of the axon initial segment. J. Comp. Neurol. *500*, 339–352.

Wimmer, V.C., Reid, C.A., Mitchell, S., Richards, K.L., Scaf, B.B., Leaw, B.T., Hill, E.L., Royeck, M., Horstmann, M.-T., Cromer, B.A., et al. (2010a). Axon initial segment dysfunction in a mouse model of genetic epilepsy with febrile seizures plus. J. Clin. Invest. *120*, 2661–2671.

Wimmer, V.C., Reid, C.A., So, E.Y.-W., Berkovic, S.F., and Petrou, S. (2010b). Axon initial segment dysfunction in epilepsy. J. Physiol. *588*, 1829–1840.

Wollner, D.A., and Catterall, W.A. (1986). Localization of sodium channels in axon hillocks and initial segments of retinal ganglion cells. Proc. Natl. Acad. Sci. USA *83*, 8424–8428.

Woodruff, A.R., Monyer, H., and Sah, P. (2006). GABAergic excitation in the basolateral amygdala. J. Neurosci. *26*, 11881–11887.

Woodruff, A.R., Anderson, S.A., and Yuste, R. (2010). The enigmatic function of chandelier cells. Front Neurosci *4*, 201.

Yu, F.H., Mantegazza, M., Westenbroek, R.E., Robbins, C.A., Kalume, F., Burton, K.A., Spain, W.J., McKnight, G.S., Scheuer, T., and Catterall, W.A. (2006). Reduced sodium current in GABAergic interneurons in a mouse model of severe myoclonic epilepsy in infancy. Nat. Neurosci. *9*, 1142–1149.

Yu, Y., Shu, Y., and McCormick, D.A. (2008). Cortical action potential backpropagation explains spike threshold variability and rapid-onset kinetics. J. Neurosci. *28*, 7260–7272.

Yu, Y., Maureira, C., Liu, X., and McCormick, D. (2010). P/Q and N channels control baseline and spike-triggered calcium levels in neocortical axons and synaptic boutons. J. Neurosci. *30*, 11858–11869.

Yue, C., and Yaari, Y. (2004). KCNQ/M channels control spike afterdepolarization and burst generation in hippocampal neurons. J. Neurosci. *24*, 4614–4624.

Zecević, D. (1996). Multiple spike-initiation zones in single neurons revealed by voltage-sensitive dyes. Nature *381*, 322–325.

Zhou, D., Lambert, S., Malen, P.L., Carpenter, S., Boland, L.M., and Bennett, V. (1998). AnkyrinG is required for clustering of voltage-gated Na channels at axon initial segments and for normal action potential firing. J. Cell Biol. *143*, 1295–1304.

Zhu, Y., Stornetta, R.L., and Zhu, J.J. (2004). Chandelier cells control excessive cortical excitation: characteristics of whisker-evoked synaptic responses of layer 2/3 nonpyramidal and pyramidal neurons. J. Neurosci. *24*, 5101–5108.